*Surface and Interface Analysis*

WILEY

SURFACE and INTERFACE ANALYSIS

RESEARCH ARTICLE OPEN ACCESS

# The Utility of Adventitious Carbon for Charge Correction: A Perspective From a Second Multiuser Facility

David J. Morgan[1,2]

[1]Cardiff Catalysis Institute, Translational Research Hub, Cardiff University, Cardiff, UK | [2]HarwellXPS, Research Complex at Harwell (RCaH), Didcot, UK

**Correspondence:** David J. Morgan (morgandj3@cardiff.ac.uk)

**Received:** 6 August 2024 | **Revised:** 2 September 2024 | **Accepted:** 11 September 2024

**Keywords:** 1s peak | adventitious carbon | binding energy reference | C 1s | charge correction | XPS

## ABSTRACT

In relation to debates in the recent literature on the utility and robustness of adventitious carbon for charge correction of X-ray photoelectron spectra, the present work explores its application using 5 years' worth of data collected by the author. The data overwhelmingly show that regardless of spectrometer or charge compensation method, and but for a few exceptions where a secondary reference is preferrable, a C 1s value of 284.8 eV is suitable for electronically isolated samples.

## 1 | Introduction

In X-ray photoelectron spectroscopy (XPS), accurate binding energies for conducting samples are readily obtained if the sample is in contact with the spectrometer. However, the majority of samples analysed are insulating, consequently during photoemission, the equilibrium potential of the surface charge will be affected by both differences in conductivity through the sample and the neutralising species; therefore, it is better to ensure such samples are electrically isolated from the spectrometer and control the surface potential using a charge compensation source. However, this raises a question: What is the best charge reference for these samples?

Charge correction is an age-old debate in the X-ray photoelectron spectroscopy community [1–3], with recent publications calling to in to question the reliability of decades worth of data [4]. Whilst it is accepted that there are both current and historically erroneous assignments in the literature, efforts are being undertaken to combat this (see, e.g., [5–7]); these are not all necessarily a consequence of poor binding energy calibration.

In recent years, Greczynski and Hultman have reviewed and proposed different methods, of calibration, including capping layers and work function measurements for vacuum level referencing [4, 8–13]. Whilst these may work in given situations, such sample preparation and measurements are impractical for a modern high-throughput analysis laboratory.

In 1982, Swift [1] reviewed the state of charge correction at the time and presented a series of published studies where the error using adventitious carbon (AdC) was no greater than ±0.4 eV, whilst Barr [14] showed this could be as good as ±0.2 eV with traceable spectrometer energy scale calibration. Recently, and based on the furore already highlighted, Biesinger has reviewed these previous works in more depth [15] and also performed a study of a large number of samples from his laboratory where the traceability of the data acquisition and analysis was known, concluding, with very few exceptions, a calibration value of 284.91 eV (with a deviation of 0.25 eV) was appropriate providing other sanity checks, such as secondary binding energy position of substrate peaks, are performed.

Whilst AdC has been used for many years for charge correction, its make-up will change in relation to the chemical nature and reactivity of the substrate (e.g., AdC on metals may differ from ceramics or oxides) and the origin of the hydrocarbons that make-up the AdC. Whilst the composition has been debated, Biesinger has also shown that AdC likely stems from volatile organic compounds (VOCs) from the atmosphere and is aliphatic

This is an open access article under the terms of the Creative Commons Attribution License, which permits use, distribution and reproduction in any medium, provided the original work is properly cited.

© 2024 The Author(s). *Surface and Interface Analysis* published by John Wiley & Sons Ltd.

in nature [16], echoing that of Barr [14]. The study also refined, through inclusion of a beta-carbon peak, the binding energy for AdC to be 284.81 eV.

This latter point raises a question on the environment in which the samples are prepared. For example, Crist has shown that the C 1s binding energy is different for metals with thick (*ca*. 10 nm) native oxides to those formed under ultra-high vacuum (UHV) [3], whilst Greczynski and Hultman have shown for Au surfaces in air, high vacuum (HV) and UHV differing levels of C, O, N and F [8], whereas the present author has not observed N or F on Au surfaces, even after prolonged exposure in HV and UHV environments. Furthermore, is a C 1s model such as that proposed by Biesinger, suitable for another laboratory, and more importantly, do the binding energies measured agree with those reported by the aforementioned laboratory?

## 2 | Experimental

The data used within this study have been acquired using two commercial XPS spectrometers. The first is a Kratos Axis Ultra DLD photoelectron spectrometer, utilising monochromatic Al kα radiation and electron-only neutralisation. High-resolution spectra were collected using pass energies of 20 or 40 eV with a 0.1 eV step. For all data used herein, sample analysis was performed in the hybrid spectroscopy mode, using the Slot aperture yielding an analysis area of *ca*. $700 \times 300\,\mu m^2$. For all samples, the X-rays were operated at a power of 120 or 144 W (10 or 12 mA × 12 kV). Samples were mounted on a double-sided adhesive tape attached to a glass slide to float them from the spectrometer.

The second system is a Thermo Fisher Scientific K-Alpha$^+$ photoelectron spectrometer, equipped with a micro-focussed monochromatic Al radiation operating at 72 W (6 mA × 12 kV) in the 400-μm spot mode, which yields an elliptical analysis area of *ca*. $600 \times 400\,\mu m^2$. Spectra were acquired at 50 eV pass energy, with a step size of 0.1 eV. Charge compensation was performed using both low energy electrons and argon ions. Samples were mounted either as for the Kratos spectrometer on glass slides or pressed into recesses of a copper powder holder plate.

The reader is reminded at this juncture that both the X-ray source and charge compensation systems can facilitate reduction of materials [17–19], which must be borne in mind when assessing the suitability of a secondary reference peak for assessing the applied charge correction methodology.

Both systems are calibrated in accordance with the ISO 15472 (2010) standard, where the instrument work function is calibrated to give an Au $4f_{7/2}$ metallic gold binding energy of 83.96 eV, and the spectrometer dispersion adjusted to give a binding energy of 932.62 eV for metallic Cu $2p_{3/2}$. By this method, the Ag $3d_{5/2}$ is reported as 368.21 eV, and all values are checked on a monthly basis.

Irrespective of system, the samples analysed are composed of a diverse range of materials, including metal oxides, hydroxides and carbonates, chlorides, 2D materials and actinide materials; graphitic materials, polymers and organics were excluded from the data set because other reference values are generally considered more suitable [20–22]. For all the spectra analysed, if excessive charging was noted, the spectra were rejected so that no bias was introduced to any fitting model based on spectral artefacts.

The spectra in this paper have originally been analysed using different versions of CasaXPS [23]. For this study, the raw data have been reanalysed using CasaXPS v2.3.26PR1.2Y. All C 1s data have been fitted using a Voigt type function characterised by the LA line shape command with the form LA(1.53,243).

## 3 | Data Analysis

For this study, data have been selected from the last 5 years during which time the analysis laboratory has relocated to new custom-built facility, thereby further investigating any influence on environmental factors. For traceability, the data selected were acquired by the author and limited to 1000 pieces of data.

Figure 1 shows the fitted C 1s spectra for materials commonly encountered within the author's laboratory, whilst Table 1 gives the peak fitting parameters used in this work. As stated, the C 1s envelope was fitted using a Voigt-like function [24], which has been shown to be more stable to variation due to noise over that of a Gaussian–Lorentzian blend peak shape (denoted as GL or SGL line shape in CasaXPS). The model was developed in-house based on the similarities noted between a large number of data sets.

As highlighted by the fitting parameters given in Table 1, whilst the model used in the present work has been independently generated, the similarities to those of Biesinger [15] are striking, with the most significant variance in the range of the C═O peak. Such differences may be a consequence, or combination, of different pass energies, environmental conditions (e.g., relative humidity, VOC's in the atmosphere) or perhaps artefacts from sample preparation by the originator of the samples. Nevertheless, both models are in good agreement, and the model presented in the present work is used throughout this paper in assessing the robustness of the AdC peak in charge correction for a range of materials. It is also interesting to note that the C 1s spectra acquired by Greczynski from a gold specimen exposed to ambient air [8] and for metals and binary compounds stored in different media [13] are also remarkably similar in shape, albeit generally fitted with an overly broad C—O signal, to those presented in Figure 1.

## 4 | Results

### 4.1 | Metal Oxides

Metal oxides are typically insulating; however, some may be semiconducting or even conductive [25]. Table 2 shows the average binding energies for several common insulating oxides taken from NIST [26], Biesinger (where reported, [27, 28]) and

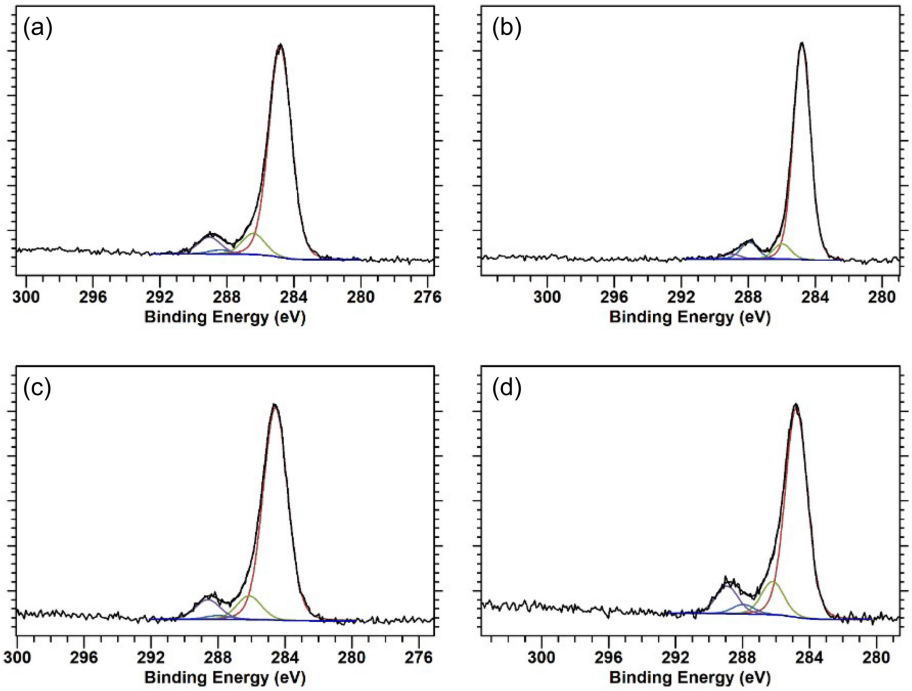


**FIGURE 1** | Fitted C 1s envelopes from (a) $TiO_2$, (b) CuS film, (c) $Pt/ZrO_2$ catalyst and (d) CuPd/ZnO catalyst.

**TABLE 1** | Adventitious carbon (AdC) C 1s fitting parameters from [15] and this work.

| | Biesinger model | | | This work | | |
|---|---|---|---|---|---|---|
| **Peak assignment** | **BE (eV)** | **Common range (eV)** | **FWHM (eV)** | **BE (eV)** | **Common range (eV)** | **FWHM (eV)** |
| C—C/C—H | 284.8 | | 0.7–1.5 | 284.8 | | 0.7–1.7 |
| C—O, C—OH | | A + 1.3 to 1.7 | A*1 | | A + 1.2 to 1.7 | A*1 |
| C═O | | A + 2.8 to 3.0 | A*1 | | A + 3.0 to 3.5 | A*1 |
| O—C═O | | A + 3.8 to 4.3 | A*1 | | A + 3.8 to 4.3 | A*1 |

the present work, all reported energies are given to the nearest 0.1 eV to match typically reported experimental step-sizes.

From Table 2, the strong correlation is noted between the binding energies in the present work and those energies reported by Biesinger. More importantly, there is an improvement over the average binding energy for a number of NIST database entries. For the present data, the highest deviation comes from that for $Al_2O_3$; however it is well known that aluminium oxides and hydroxides are notoriously difficult to distinguish due to the uncertainty in the chemical composition of samples recorded and the statistical deviation between these compounds [26]; however, both the reported binding energy and deviation is in good agreement with that for thin film alumina grown on silica [29–31] and a well-defined sample of ɣ-$Al_2O_3$ [32].

## 4.2 | Carbonates and Salts

To further check the validity of the carbon model, several reference salts and carbonates were analysed in the 5-year period. Table 3 shows a sample of carbonates recorded by the author, together with references where available from NIST and the datasets provided by Crist [33] as a further reference point, whilst Table 4 shows a sample of chloride salts.

For the salts, there is an excellent agreement with those of NIST, with the largest difference (0.4 eV) noted for $YCl_3$. Such differences may be a consequence of the level of hydration or duration of analysis, with an identical binding energy difference observed during the analysis of $RuCl_3$ [34].

For the carbonates, the consensus between the binding energies is good, with an average binding energy for the $CO_3$ fragment found to be 289.6 eV, with a deviation of 0.16 eV. This average excludes potassium carbonate where the binding energy is *ca.* 1 eV below the average value but is consistent with published data [26, 35]. With the exception of potassium carbonate, the use of the $CO_3$ peak, as a secondary calibration reference perhaps suitable for materials, such as those containing zirconium and hafnium, which depending on how stored, can reveal a significant carbonate signal [13].

**TABLE 2** | Comparison of binding energies from NIST, Biesinger and the present work for a selection of metal oxides.

| | | Binding energy/eV (ref. to 284.8 eV) | | |
|---|---|---|---|---|
| **Compound** | **Core level** | **Average NIST (std. dev)** | **Biesinger (std. dev)** | **This work (std. dev)** |
| $TiO_2$ (P25) | Ti $2p_{3/2}$ | 458.7 (0.2) | N.R. | 458.7 (0.1) |
| $TiO_2$ (anatase) | | 458.7 (0.1) | 458.6 (0.0) | 458.8 (0.1) |
| $TiO_2$ (rutile) | | 459.0 (n/a) | 458.5 (0.1) | 458.7 (0.1) |
| $SiO_2$ | Si 2p | 103.5 (0.3) | N.R. | 103.4 (0.1) |
| ɣ-$Fe_2O_3$[a] | Fe $2p_{3/2}$ | 710.9 (0.4) | 710.8 (0.1) | 710.8 (0.2) |
| $Nb_2O_5$ | Nb $3d_{5/2}$ | 207.4 (0.4) | N.R. | 207.2 (0.1) |
| $ZrO_2$ | Zr $3d_{5/2}$ | 182.8 (0.6) | N.R. | 182.2 (0.17) |
| $Al_2O_3$ | Al 2p | 74.1 (1.0) | N.R. | 74.8 (0.3) |
| $ZnO_2$ | Zn $2p_{3/2}$ | 1021.7 (0.4) | 1021.0 (0.04) | 1021.1 (0.05) |

Abbreviation: NR = not reported.
[a]Value taken from the second peak as fitted using Gupta and Sen multiplet values, which also corresponds roughly to the peak maximum for ɣ-$Fe_2O_3$ where most users will read the binding energy.

**TABLE 3** | Carbonate ($CO_3$) moiety binding energies for a range of metal carbonates relative to AdC at 284.8 eV.

| | | $CO_3$ binding energy/eV (ref to 284.8 eV) | | | |
|---|---|---|---|---|---|
| **Compound** | **Core level** | **Average NIST (std. dev)** | **Crist[a]** | **This work (std. dev)** | **Core level BE (eV)** |
| $K_2CO_3$ | K $2p_{3/2}$ | N.R. | 288.5 | 288.5 (0.2) | 292.6 |
| $Li_2CO_3$ | Li 1s | 289.7 (0.13) | 289.8 | 289.8 (0.1) | 55.2 |
| $Ba_2CO_3$ | Ba $3d_{5/2}$ | 289.6 (0.7) | 289.3 | 289.5 (0.2) | 779.9 |
| $NiCO_3$ | Ni $2p_{3/2}$ | N.R. | 289.6 | 289.8 (0.2) | 856.3 |
| $CoCO_3$ | Co $2p_{3/2}$ | 289.4 | 289.8 | 289.4 (0.15) | 781.1 |
| $MnCO_3$ | Mn $2p_{3/2}$ | N.R. | 289.6 | 289.8 (0.2) | 641.5 |
| $CaCO_3$ | Ca $2p_{3/2}$ | 289.6 (0.3) | 289.8 | 289.6 (0.2) | 347.0 |

Abbreviation: N.R. = binding energy not reported.
[a]No deviation reported as only single measurements present in dataset.

**TABLE 4** | Cl$2p_{3/2}$ binding energies for some metal chlorides relative to AdC at 284.8 eV.

| | | | | Binding energy/eV (ref to 284.8 eV) | |
|---|---|---|---|---|---|
| | | | | This work | |
| **Compound** | **Metallic core level** | **Average metallic core level BE (eV) NIST[a] (std. dev)** | **Average Cl $2p_{3/2}$ NIST[a] (std. dev)** | **Cl $2p_{3/2}$ (std. dev)** | **Metallic core level BE (eV)** |
| NaCl | Na 1s | 1071.5 (0.2) | 198.5 (0.3) | 198.6 (0.08) | 1071.7 (0.05) |
| KCl | K $2p_{3/2}$ | 292.7 (0.16) | 198.2 (0.2) | 198.2 (0.05) | 292.8 (0.05) |
| $YCl_3$ | Y 4d | 186.6 (0.0) | 199.3 (0.0) | 198.9 (0.1) | 186.7 (0.1) |

[a]Average and standard deviation calculated with significant outliers ignored. If included, average is 196.9 eV, with a deviation of 2.6 eV for NaCl and 196.2 with a deviation of 2.8 eV for KCl.

### 4.3 | Effect of Charge Compensation System and Obtaining a Constant Surface Charge State

The two photoelectron spectrometers employed within this study offer two distinct methods of charge compensation, specifically low energy electrons only (Kratos) and combined dual low-energy argon ions and electrons (Thermo). For a more detailed discussion on charge compensation systems and their utility, the reader is directed to [36, 37]. However, between both systems, no observable difference in peak position or reproducibility was observed during analysis.

What was observable in comparing the data and subsequent testing was the time to obtain a stable surface potential through charge compensation. To illustrate this, Figure 2 shows a series of 0.5 wt% Pd/$TiO_2$ catalysts, which have undergone different reaction times.

It is evident from Figure 2a the first set of Ti 2p spectra vary in position by approximately 1.0 eV, whereas the difference in Figure 2b is 0.5 eV. It is notable for the equivalently coloured spectra that with increased analysis time, the spectra become more stable and are attributed to a more uniform charge potential at the surface, a supposition supported by the unexpected ratio differences in the Ti$2p_{3/2}$ and $2p_{1/2}$ peaks in Figure 2a, suggesting some degree of initial charging. Of course, the spectra in Figure 2b still show some variance between peak maxima; this however invokes one of the points which Biesinger highlights, specifically confirming calibration by a secondary peak—in this case, the Ti $2p_{3/2}$ signal. Such secondary references are useful, especially in areas such as catalytic science, where the surface chemistry will undoubtedly change due to preparation methods and reactions. Of course, in this example, the Ti $2p_{3/2}$ signal is a valid option, as the titanium remains in its oxidic, 4+ state. Unless evidence exists, such as that from Raman or XRD, that some significant change has occurred that may influence the recorded core-level binding energies of the support material, then the titania is not expected to change position outside of any experimental error.

This also highlights a common error amongst newer analysts—ignoring variability in X-ray performance. This is perhaps especially true with the advent of more 'walk-up and analyse' XPS instrumentation where spectral acquisition can begin in under 30 min after sample insertion. Ideally, before any analysis, an XPS system should have a period where both X-ray and charge compensation sources have a time to 'warm-up' and equilibrate, thus providing a more stable flux from each source reaching the sample. A more detailed discussion on variability in XPS is detailed by Shard [38]. For clarity, for recording the spectra in Figure 2, the sources were allowed to warm-up for 60 min before analysis began, suggesting the variance noted is a consequence of achieving a stable surface potential, although achievement of this due to desorption of some AdC is not discounted.

In reviewing the data used in this study, it was evident that secondary reference point was required in a small number of cases. This may be a result of the C 1s line being weak (typical for many $SiO_2$ samples) or noting an unacceptable shift in the core level after C 1s calibration after reaction or heat treatment (as already discussed for $TiO_2$).

Such phenomena can be related to a change in the concentration of surface species such as hydroxyl groups, or changes in surface acidity/basicity and can be demonstrated by aluminosilicates (zeolites). For example, as the Si/Al ratio in zeolites increases, acidity decreases indicating the aluminium is introducing Brønstead acid character [39]. It is not unfathomable; therefore, the interaction between any carbonaceous surface species will interact differently with surfaces exhibiting different levels of acidity.

An example of this is given in Figure 3, where a series of ZSM-5 zeolites with differing $SiO_2/Al_2O_3$ mole ratios (23, 50, 80 and 280) have been analysed. Figure 3a,b shows the Si 2p and Al 2p peaks calibrated to the Si 2p line taken to be 103.5 eV, whilst panels (c) and (d) show the spectra calibrated to the C 1s signal at 284.8 eV, where the variability is greater than an expected experimental uncertainty of *ca*. 0.2 eV. It does not go unnoticed that in calibrating the Si 2p peak, the variance in the Al 2p peak is greater between the high and low Si/Al ratios (difference *ca*. 0.9 eV) than in comparison with C 1s calibration, where the difference is *ca*. 0.5 eV and identical to the shift in the Si 2p, whilst calibration to the Al 2p, taken to be 74.8 eV (see Table 2), results in a deviation in Si 2p energies of 0.9 eV and C 1s energies of 0.5 eV. The differences in Al 2p and Si 2p binding energies if calibrated to carbon have been related to the increased charge in the zeolite being distributed unevenly around $SiO_4$ and $AlO_4$ units [40]; however, irrespective of these observations, it is clear that the Si 2p peak in this situation can be considered a more suitable reference given the concentration of $SiO_4$ units present and therefore more comparable to bulk $SiO_2$.

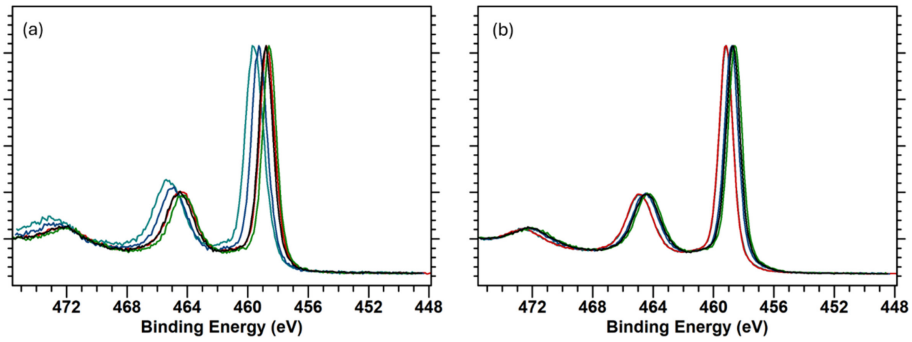


**FIGURE 2** | Ti 2p core-level spectra for a series of 0.5 wt% Pd/$TiO_2$ catalyst samples where (a) spectra recorded immediately from determining analysis height (x1 scan) and (b) later in the same experimental flow (×6 scans). The acquisition time for each sweep is approximately 10 s and (b) was recorded approximately 1500 s (25 min) later.

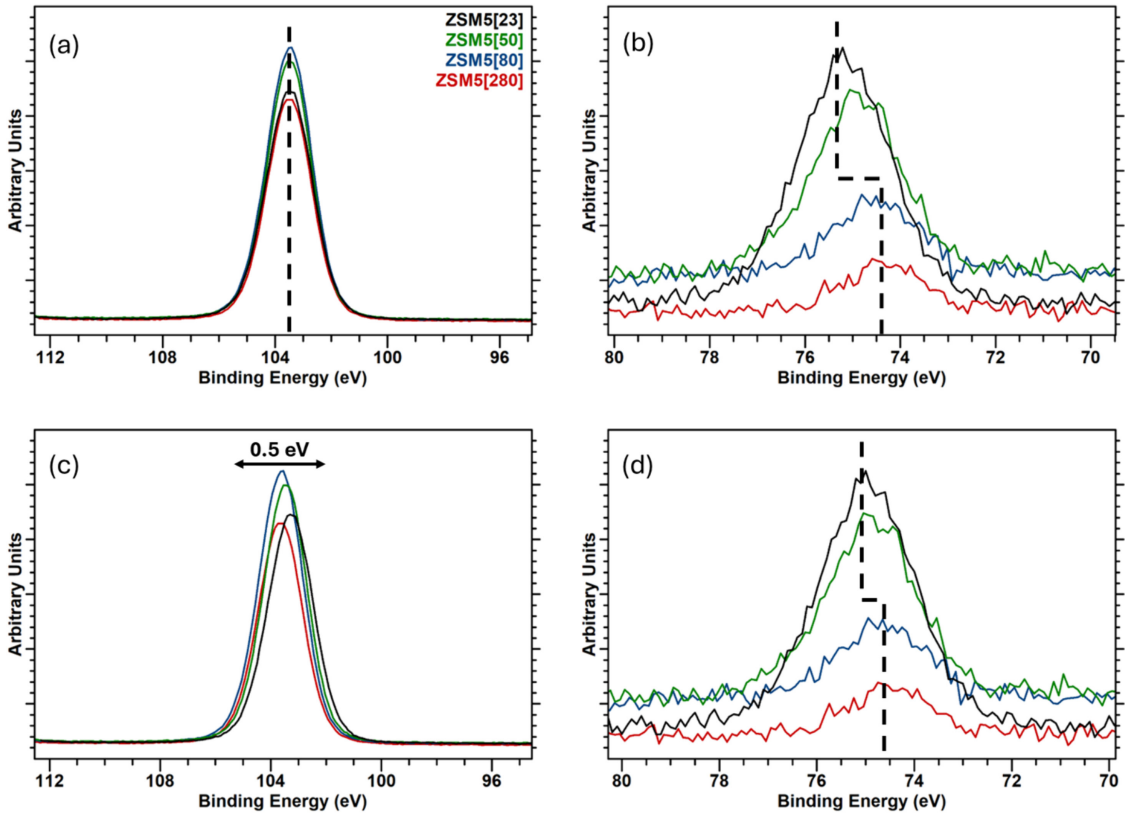


**FIGURE 3** | Si 2p and Al 2p core level spectra for a series of ZSM-5 samples with differing $SiO_2/Al_2O_3$ mole ratios, where panels (a) and (b) are calibrated to the Si 2p peak, whilst panels (c) and (d) are calibrated to the C 1s peak.

Evident from the aluminosilicate data is that differences can exist between environments within a sample, even in the absence of charging effects. In such cases, whilst a secondary reference is generally suitable, there may be instances where the energetic difference between two photoemission peaks is preferable to infer chemistry. Such differences may be the difference between Auger and photoemission core-lines (the Auger parameter), which is independent of both charging and reference levels effects [41–43], or the difference between two core-lines, such O 1s and the principle metal core-line, which has been used to determine reliable chemical state identification for a series of niobates [44] and titanium containing oxides [45].

## 5 | Conclusions

The data and discussion presented herein, in addition to that of Biesinger [15], illustrate that adventitious carbon, found on air-exposed samples, is a valid method of calibration providing care is taken during data analysis. Despite some variation in peak fitting parameters, the present model and that previously reported are in excellent agreement, with differences likely due to environmental factors. Moreover, despite differences in fitting methodology, the shape of the spectral envelope to carbon species reported by Greczynski and Hultman for gold and aluminium [8, 9] is also in excellent agreement. These observations suggest, regardless of the environment, that similar C 1s envelopes are expected.

Whilst AdC referencing has been reported to yield a 95% success rate [15], there will always be exceptions, or preferred alternatives to AdC referencing. For example, polymers are still better suited to calibration to 285 eV for comparison with Beamson and Briggs [20], whilst samples contaminated with siloxanes such as polydimethylsiloxane (PDMS), where the C 1s peak is reported at 284.4 eV [46], and similarly where there is a high degree of graphitic carbon (C 1s = 284.5 eV, [22]), or for conductors the Fermi edge, providing it has sufficient intensity, are undoubtedly a good choice.

Discussion has already been made on changes in surface chemistry due to reaction of heat treatment affecting the interaction of carbon with the surface (see $TiO_2$ and aluminosilicates), so the use of a known and stable secondary reference, such as a support material, metal peak or fermi edge, if the sample is conducting, is critical.

Ultimately, for the majority of XPS analysis where samples are electrically isolated from the spectrometer, charge referencing using a value of 284.8 eV for adventitious carbon is still the most appropriate choice, providing the advice presented herein and in [15] is followed.

### Data Availability Statement

Data sharing not applicable - no new data generated.

**References**


1. P. Swift, "Adventitious Carbon—The Panacea for Energy Referencing?," *Surface and Interface Analysis* 4 (1982): 47–51, https://doi.org/10.1002/sia.740040204.

2. R. J. Bird and P. Swift, "Energy Calibration in Electron Spectroscopy and the Re-Determination of Some Reference electron Binding Energies," *Journal of Electron Spectroscopy and Related Phenomena* 21 (1980): 227–240, https://doi.org/10.1016/0368-2048(80)85050-X.

3. B. V. Crist, "XPS in Industry—Problems With Binding Energies in Journals and Binding Energy Databases," *Journal of Electron Spectroscopy and Related Phenomena* 231 (2019): 75–87, https://doi.org/10.1016/j.elspec.2018.02.005.

4. G. Greczynski and L. Hultman, "Compromising Science by Ignorant Instrument Calibration—Need to Revisit Half a Century of Published XPS Data," *Angewandte Chemie, International Edition* 59 (2020): 5002–5006, https://doi.org/10.1002/anie.201916000.

5. D. R. Baer, G. E. McGuire, K. Artyushkova, C. D. Easton, M. H. Engelhard, and A. G. Shard, "Introduction to Topical Collection: Reproducibility Challenges and Solutions With a Focus on Guides to XPS Analysis," *Journal of Vacuum Science and Technology A* 39 (2021): 021601, https://doi.org/10.1116/6.0000873.

6. M. H. Engelhard, D. R. Baer, A. Herrera-Gomez, and P. M. A. Sherwood, "Introductory Guide to Backgrounds in XPS Spectra and Their Impact on Determining Peak Intensities," *Journal of Vacuum Science and Technology A* 38 (2020): 063203, https://doi.org/10.1116/6.0000359.

7. D. R. Baer, K. Artyushkova, C. Richard Brundle, et al., "Practical Guides for X-Ray Photoelectron Spectroscopy: First Steps in Planning, Conducting, and Reporting XPS Measurements," *Journal of Vacuum Science and Technology A* 37 (2019): 031401, https://doi.org/10.1116/1.5065501.

8. G. Greczynski and L. Hultman, "X-Ray Photoelectron Spectroscopy: Towards Reliable Binding Energy Referencing," *Progress in Materials Science* 107 (2020): 100591, https://doi.org/10.1016/j.pmatsci.2019.100591.

9. G. Greczynski and L. Hultman, "The Same Chemical State of Carbon Gives Rise to Two Peaks in X-Ray Photoelectron Spectroscopy," *Scientific Reports* 11 (2021): 11195, https://doi.org/10.1038/s41598-021-90780-9.

10. G. Greczynski, O. Pshyk, and L. Hultman, "Toward an Increased Reliability of Chemical Bonding Assignment in Insulating Samples by X-Ray Photoelectron Spectroscopy," *Science Advances* 9 (2023): eadi3192, https://doi.org/10.1126/sciadv.adi3192.

11. G. Greczynski and L. Hultman, "C 1s Peak of Adventitious Carbon Aligns to the Vacuum Level: Dire Consequences for Material's Bonding Assignment by Photoelectron Spectroscopy," *ChemPhysChem* 18 (2017): 1507–1512, https://doi.org/10.1002/cphc.201700126.

12. G. Greczynski and L. Hultman, "Reliable Determination of Chemical State in X-Ray Photoelectron Spectroscopy Based on Sample-Work-Function Referencing to Adventitious Carbon: Resolving the Myth of Apparent Constant Binding Energy of the C 1s Peak," *Applied Surface Science* 451 (2018): 99–103, https://doi.org/10.1016/j.apsusc.2018.04.226.

13. G. Greczynski and L. Hultman, "Impact of Sample Storage Type on Adventitious Carbon and Native Oxide Growth: X-Ray Photoelectron Spectroscopy Study," *Vacuum* 205 (2022): 111463, https://doi.org/10.1016/j.vacuum.2022.111463.

14. T. L. Barr and S. Seal, "Nature of the Use of Adventitious Carbon as a Binding Energy Standard," *Journal of Vacuum Science & Technology, A: Vacuum, Surfaces, and Films* 13 (1995): 1239–1246, https://doi.org/10.1116/1.579868.

15. M. C. Biesinger, "Accessing the Robustness of Adventitious Carbon for Charge Referencing (Correction) Purposes in XPS Analysis: Insights From a Multi-User Facility Data Review," *Applied Surface Science* 597 (2022): 153681, https://doi.org/10.1016/j.apsusc.2022.153681.

16. L. H. Grey, H. Y. Nie, and M. C. Biesinger, "Defining the Nature of Adventitious Carbon and Improving Its Merit as a Charge Correction Reference for XPS," *Applied Surface Science* 653 (2024): 159319, https://doi.org/10.1016/j.apsusc.2024.159319.

17. L. Edwards, P. Mack, and D. J. Morgan, "Recent Advances in Dual Mode Charge Compensation for XPS Analysis," *Surface and Interface Analysis* 51 (2019): 925–933, https://doi.org/10.1002/sia.6680.

18. R. L. McLaren, G. R. Owen, and D. J. Morgan, "Analysis Induced Reduction of a Polyelectrolyte," *Results in Surfaces and Interfaces* 6 (2022): 100032, https://doi.org/10.1016/j.rsurfi.2021.100032.

19. D. J. Morgan, "XPS Insights: Sample Degradation in X-Ray Photoelectron Spectroscopy," *Surface and Interface Analysis* 55 (2023): 331–335, https://doi.org/10.1002/sia.7205.

20. G. Beamson and D. Briggs, *High Resolution XPS of Organic Polymers: The Scienta ESCA300 Database* (Chichester, UK: Wiley-Blackwell, 1992).

21. D. J. Morgan, "Cluster Cleaned HOPG by XPS," *Surface Science Spectra* 24, no. 2 (2017): 024003, https://doi.org/10.1116/1.4993771.

22. D. J. Morgan, "Comments on the XPS Analysis of Carbon Materials," C (2021), 7. https://doi.org/10.3390/c7030051.

23. N. Fairley, V. Fernandez, M. Richard-Plouet, et al., "Systematic and Collaborative Approach to Problem Solving Using X-Ray Photoelectron Spectroscopy," *Applied Surface Science Advances* 5 (2021): 100112, https://doi.org/10.1016/j.apsadv.2021.100112.

24. G. H. Major, T. G. Avval, D. I. Patel, et al., "A Discussion of Approaches for Fitting Asymmetric Signals in X-Ray Photoelectron Spectroscopy (XPS), Noting the Importance of Voigt-Like Peak Shapes," *Surface and Interface Analysis* 53 (2021): 689–707, https://doi.org/10.1002/sia.6958.

25. D. J. Morgan, "XPS Insights: Asymmetric Peak Shapes in XPS," *Surface and Interface Analysis* 55 (2023): 567–571, https://doi.org/10.1002/sia.7215.

26. C. D. Wagner, A. V. Naumkin, A. Kraut-Vass, J. W. Allison, C. J. Powel, and J. R. Rumble, "NIST Standard Reference Database 20, Version 3.4 (Web Version)," (2003), accessed 06 August 2024, http://srdata.nist.gov/xps/, https://doi.org/10.18434/T4T88K.

27. M. C. Biesinger, L. W. Lau, A. R. Gerson, and R. S. Smart, "Resolving Surface Chemical States in XPS Analysis of First Row Transition Metals, Oxides and Hydroxides: Sc, Ti, V, Cu and Zn," *Applied Surface Science* 257, no. 3 (2010): 887–898, https://doi.org/10.1016/j.apsusc.2010.07.086.

28. M. C. Biesinger, B. P. Payne, A. P. Grosvenor, L. W. Lau, A. R. Gerson, and R. S. Smart, "Resolving Surface Chemical States in XPS Analysis of First Row Transition Metals, Oxides and Hydroxides: Cr, Mn, Fe, Co and Ni," *Applied Surface Science* 257, no. 7 (2011): 2717–2730, https://doi.org/10.1016/j.apsusc.2010.10.051.

29. N. Madaan, S. S. Kanyal, D. S. Jensen, et al., "$Al_2O_3$ e-Beam Evaporated Onto Silicon (100)/$SiO_2$, by XPS," *Surface Science Spectra* 20, no. 1 (2013): 43–48, https://doi.org/10.1116/11.20121102.

30. K. J. Kim, J. S. Jang, J. H. Lee, Y. J. Jee, and C. S. Jun, "Determination of the Absolute Thickness of Ultrathin $Al_2O_3$ Overlayers on Si (100) Substrate," *Analytical Chemistry* 81 (2009): 8519–8522, https://doi.org/10.1021/ac901463m.

31. P. Boryło, K. Lukaszkowicz, M. Szindler, et al., "Structure and Properties of $Al_2O_3$ Thin Films Deposited by ALD Process," *Vacuum* 131 (2016): 319–326, https://doi.org/10.1016/j.vacuum.2016.07.013.

32. B. R. Strohmeier, "Gamma-Alumina ($\gamma$-$Al_2O_3$) by XPS," *Surface Science Spectra* 3, no. 2 (1994): 135–140, https://doi.org/10.1116/1.1247774.

33. B. V. Crist, accessed 06 August 2024, www.xpslibrary.com.

34. D. J. Morgan, "Resolving Ruthenium: XPS Studies of Common Ruthenium Materials," *Surface and Interface Analysis* 47 (2015): 1072–1079, https://doi.org/10.1002/sia.5852.

35. A. Shchukarev and D. Korolkov, "XPS Study of Group IA Carbonates," *Open Chemistry* 2 (2004): 347–362, https://doi.org/10.2478/BF02475578.

36. D. R. Baer, K. Artyushkova, H. Cohen, et al., "XPS Guide: Charge Neutralization and Binding Energy Referencing for Insulating Samples," *Journal of Vacuum Science and Technology A* 38 (2020): 031204, https://doi.org/10.1116/6.0000057.

37. D. J. Morgan, "XPS Analysis of Electrically Insulating Catalytic Materials," (2023): 97–120, https://doi.org/10.1142/9781800613294_0005.

38. A. G. Shard, "Practical Guides for X-Ray Photoelectron Spectroscopy: Quantitative XPS," *Journal of Vacuum Science and Technology A* 38 (2020): 041201, https://doi.org/10.1116/1.5141395.

39. A. S. Al-Dughaither and H. de Lasa, "HZSM-5 Zeolites With Different $SiO_2/Al_2O_3$ Ratios. Characterization and $NH_3$ Desorption Kinetics," *Industrial and Engineering Chemistry Research* 53 (2014): 15303–15316, https://doi.org/10.1021/ie4039532.

40. O. L. J. Gijzeman, A. J. M. Mens, J. H. van Lenthe, W. J. Mortier, and B. M. Weckhuysen, "The Effect of Chemical Composition and Structure on XPS Binding Energies in Zeolites," *Journal of Physical Chemistry B* 107 (2003): 678–684, https://doi.org/10.1021/jp021948d.

41. G. Moretti, "Auger Parameter and Wagner Plot in the Characterization of Chemical States by X-Ray Photoelectron Spectroscopy: A Review," *Journal of Electron Spectroscopy and Related Phenomena* 95 (1998): 95–144, https://doi.org/10.1016/s0368-2048(98)00249-7.

42. G. Moretti, "The Wagner Plot and the Auger Parameter as Tools to Separate Initial- and Final-State Contributions in X-Ray Photoemission Spectroscopy," *Surface Science* 618 (2013): 3–11, https://doi.org/10.1016/j.susc.2013.09.009.

43. J. L. Bourque, M. C. Biesinger, and K. M. Baines, "Chemical State Determination of Molecular Gallium Compounds Using XPS," *Dalton Transactions* 45 (2016): 7678–7696, https://doi.org/10.1039/C6DT00771F.

44. V. V. Atuchin, I. E. Kalabin, V. G. Kesler, and N. V. Pervukhina, "Nb 3d and O 1s Core Levels and Chemical Bonding in Niobates," *Journal of Electron Spectroscopy and Related Phenomena* 142 (2005): 129–134, https://doi.org/10.1016/j.elspec.2004.10.003.

45. V. V. Atuchin, V. G. Kesler, N. V. Pervukhina, and Z. Zhang, "Ti 2p and O 1s Core Levels and Chemical Bonding in Titanium-Bearing Oxides," *Journal of Electron Spectroscopy and Related Phenomena* 152 (2006): 18–24, https://doi.org/10.1016/j.elspec.2006.02.004.

46. P. Louette, F. Bodino, and J. J. Pireaux, "Poly (Dimethyl Siloxane) (PDMS) XPS Reference Core Level and Energy Loss Spectra," *Surface Science Spectra* 12, no. 1 (2005): 38–43, https://doi.org/10.1116/11.20050908.